Solid State Ionics 180 (2009) 222–225

Contents lists available at ScienceDirect

Solid State Ionics

journal homepage: www.elsevier.com/locate/ssi

Determination of the diffusion coefficient of lithium ions in nano-Si

N. Ding [a,b], J. Xu [a], Y.X. Yao [a], G. Wegner [b], X. Fang [a], C.H. Chen [a,*], I. Lieberwirth [b,*]

[a] Department of Materials Science and Engineering, University of Science and Technology of China, Anhui Hefei 230026, China
[b] Max Planck Institute for Polymer Research, Mainz, 55128, Germany

ARTICLE INFO

Article history:
Received 29 September 2008
Received in revised form 9 December 2008
Accepted 10 December 2008

Keywords:
Lithium diffusion
Silicon
Impedance spectroscopy
Galvanostatic intermittent titration
Li-ion battery

ABSTRACT

The diffusion coefficients of lithium ions (D_{Li^+}) in nano-Si were determined by cyclic voltammetry (CV), electrochemical impedance spectroscopy (EIS) and galvanostatic intermittent titration technique (GITT). D_{Li^+} values are estimated to be ~10^{-12} cm^2 s^{-1} and exhibit a "W" type varying with the lithium concentration in silicon. Two minimum regions of D_{Li^+} (at $Li_{2.1\pm0.2}Si$ and $Li_{3.2\pm0.2}Si$) are found, which probably result from two amorphous compositions (a-Li_7Si_3 and a-$Li_{13}Si_4$). Besides the two minimum regions, one maximum D_{Li^+} is observed at $Li_{15}Si_4$, corresponding to the crystallization of highly lithiated amorphous Li_xSi.

1. Introduction

Li-ion batteries are widely used in electronic portable devices. Since Li metal as anode material suffers from the effect of forming undesirable dendrites and thus accompanies safety problems, graphite is the dominating anode material in commercial batteries. However, the theoretical specific capacity (QT) of graphite is only 372 mA h g^{-1}. In addition, to increase the batteries' energy density, anode materials with higher capacity are also needed. Among all anode materials, silicon is the best candidate to meet these requirements, whose QT can reach more than 4000 mA h g^{-1} [1].

Silicon as the anode of Li-ion batteries has been investigated for more than 30 years [2]. Two periods of time can be distinguished, the first period is in the early development of Li-ion batteries since the 1970s, the other period is after 1994, following the patents announcement by Fujifilm [3,4]. At its early stage, the batteries had to be operated at around 400 °C. At the high temperature, silicon forms four different phases $Li_{12}Si_7$, Li_7Si_3, $Li_{13}Si_4$ and $Li_{21}Si_5$ with the degree of lithium intercalation [5]. In the recent 10 years, the studies on silicon as anode material have been concentrated on batteries working at the room temperature [6–10]. At the room temperature, silicon shows a different intercalation process: the crystalline silicon initially transforms into an amorphous lithiated silicon phase during lithium intercalation when the voltage is above 0.06 V (vs. Li^+/Li), and below 0.06 V a new crystalline phase of $Li_{15}Si_4$ was observed [11]. In the whole intercalation process, the silicon undergoes 300% volume inflation. The large volume change can cause the mechanical failure and leads to the capacity fading. A series of studies have reported that silicon–carbon composites and amorphous silicon exhibit a better cycling performance than crystalline silicon [12–17]. However, the transport kinetics of lithium in silicon is still unclear. Cyclic voltammetry (CV), electrochemical impedance spectroscopy (EIS), galvanostatic intermittent titration technique (GITT) and potentiostatic intermittent titration technique (PITT) have been widely applied to estimate the diffusion coefficients of lithium ions (D_{Li^+}) in the electrodes (assuming that electronic charge carriers have much higher diffusivities than the lithium ions) [18–20]. Recently, Kulova et al. have reported that D_{Li^+} in amorphous Si:H at the potential of 0.01 V (vs. Li^+/Li) is $(2–3)\times10^{-13}$ cm^2 s^{-1} [21]. However, D_{Li^+} in crystalline silicon at different charge–discharge states at room temperature is still not available. In this study, CV, EIS and GITT were applied to estimate the diffusion coefficients of lithium ions in nano-Si.

2. Experimental

Nano-Si powder (Aldrich, 98%, average particle size: 50 nm) was used as an anode material. Transmission electron microscopy (TEM) was conducted to study the microstructure of the electrode with a FEI TECNAI F20 microscope operated at 200 keV. The electrode was comprised of 40 wt.% nano-Si, 40 wt.% carbon black and 30 wt.% sodium carboxymethyl cellulose (pH=3.5, in 5 wt.% distilled water, adjusted by formic acid). The electrolyte was a solution of 1 M $LiPF_6$ dissolved in EC/DEC (1:1 (w/w)) where EC and DEC stand for ethylene carbonate and diethyl carbonate, respectively. Lithium metal was chosen as the counter electrode. Coin cells (CR 2032 type) were

* Corresponding authors. Chen is to be contacted at Tel.: +86 551 3606971; fax: +86 551 3601592. Lieberwirth, Tel.: +49 6131 379580; fax: +49 6131 379100.
E-mail addresses: cchchen@ustc.edu.cn (C.H. Chen), lieberw@mpip-mainz.mpg.de (I. Lieberwirth).

0167-2738/$ – see front matter © 2008 Elsevier B.V. All rights reserved.
doi:10.1016/j.ssi.2008.12.015

assembled in an argon-filled dry-box (MBraun Labmaster 130) with a porous polypropylene membrane (Celgard 2400) as the separator.

The cells were discharged on a multi-channel battery system (NewareBTS2300, Shenzhen) at a constant current of 0.2 mA cm^{-2}. Cyclic Voltammetry (CV) and electrochemical impedance spectra (EIS) at different charge–discharge states were measured on CHI 604 Electrochemical Workstation in the frequency range from 100 kHz to 100 mHz. In order to realize an equilibrium state, all cells for EIS were stabilized for 30 min before measurement. The galvanostatic intermittent titration technique (GITT) was employed at a pulse of 50 mA g^{-1} for 7 min and with 10 min interruption between each pulse.

3. Results and discussion

The TEM and HRTEM images of nano-Si are shown in Fig. 1. The particles are quite uniform in size and well crystalline. The lattice distance of (111) is calculated from the diffraction pattern to be 3.13 Å. Silicon has a cubic symmetry (diamond structure, $Z=8$), therefore it is easy to calculate its unit cell parameter ($a=5.42$ Å) and the molar volume ($V_M=11.99$ cm^3 mol^{-1}).

The galvanostatic charge–discharge curves of nano-Si are shown in Fig. 2. To enhance the cyclability, the electrode was mixed with 40 wt.% carbon black, whose discharge capacity can reach about 400 mA h g^{-1} in the first cycle, therefore, the apparent discharge capacity of the electrode is beyond the theoretical capacity of nano-Si ($Li_{4.2}Si$). To remove the influence of carbon black (undergoing a large initial irreversible capacity loss), the subsequent charge–discharge curve is used to estimate the diffusion coefficient and the final composition of the second discharge curve is normalized into $Li_{4.2}Si$. The voltage profiles exhibit two distinct regions and the differentiation curves show two maximum peaks at about $Li_{2.1}Si$ and $Li_{3.2}Si$, respectively (see the inset in Fig. 2). The presence of these two regions with different plateaus indicates that x in amorphous phase Li_xSi does not change smoothly; there must be other two amorphous phases, such as a-Li_7Si_3 and a-$Li_{13}Si_4$. And with the x range from 2.2 to 3.1, there is a long slope, indicating that Li reacts with Li_xSi forming a solid solution. In addition, when the voltage is below 0.05 V, the discharge curve exhibits another plateau, which corresponds to a composition of roughly $Li_{3.8}Si$ resulting from the formation of crystalline $Li_{15}Si_4$.

Fig. 3a shows the CV curves with different scan rates. If the charge transfer at the interface is fast enough and the restrain process is the lithium diffusion in electrode, the relationship of the peak current and the CV sweep rate is:

$$i_p = \left(2.69\times10^5\right) n^{3/2} A D_{Li^+}^{1/2} C_{Li}^{*} v^{1/2} \quad (1)$$

where i_p is the peak current (A), n is the charge concentration in Li_xSi (as the first reduction peak is chosen in calculation, $n=2.2$), A is the contact area between Si and electrolyte (here the geometric area of electrode, 1.54 cm^2, is used for simplicity), C_{Li}^{*} is the bulk concentration of lithium in electrode (0.0753 mol cm^{-3}, calculated from Li_7Si_3), and v is the scan rate. The peak current has a linear relationship with the square root of scan rate according to Eq. (1) (as shown in Fig. 3b). D_{Li^+} in nano-Si is estimated to be 5.1×10^{-12} cm^2 s^{-1} after a preliminary calculation. This value is higher than the diffusion coefficient of free dilute Li^+ in bulk Si, where D_{Li^+} is 3×10^{-14} cm^2 s^{-1} [22]. The biggest difference is with the contact area (A) used for calculation. In a bulk or thin film situation, it is easy to know that the contact area is roughly the same as its geometric area of the sample. But in our case, the real contact area must be significantly higher than the geometric area, which is used for calculation. Therefore, the absolute values obtained here are the "apparent diffusion coefficient", which is greater than the real one.

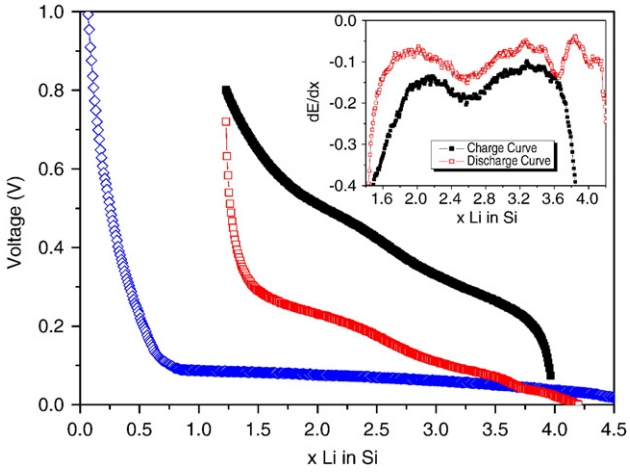

Fig. 2. Galvanostatic charge–discharge curves of nano-Si, cycled at a constant current of 0.2 mA cm^{-2}.

The Nyquist plots at different charge states are shown in Fig. 4. The plots consist of one or two depressed semicircles in the high- and intermediate-frequency region and the Warburg-type element (the sloping line) in the low-frequency region, respectively. The first semicircle results from the solid electrolyte interface forming at the interface between electrolyte and electrode, which is stable and does not change too much during charge and discharge, whereas the second semicircle, corresponding to charge transfer, increases from 7 Ω (at full charge state) to 120 Ω (at full discharge state, data not shown in Fig. 4). The large impedance at full discharge state is probably related to the deposition of lithium on the silicon surface.

Warburg impedance corresponds to the lithium diffusion in nano-Si, therefore the Warburg part can be used to calculate D_{Li^+} by using

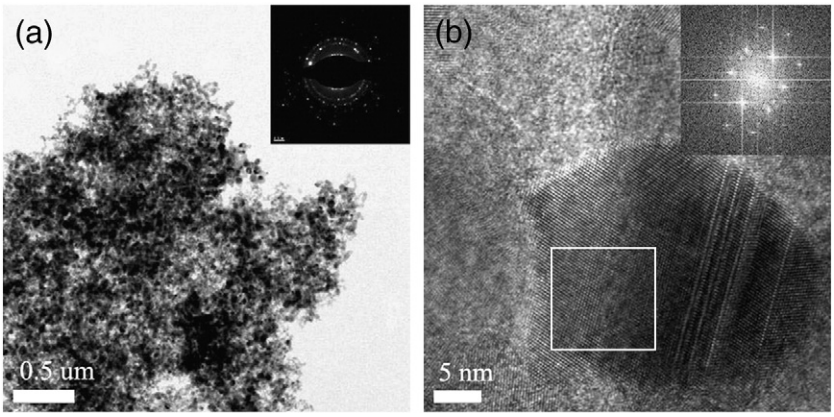

Fig. 1. (a) TEM and (b) HRTEM images of nano-Si. The electron diffraction pattern and fast Fourier transforms of the selected area in HRTEM image are present on the top right corner.

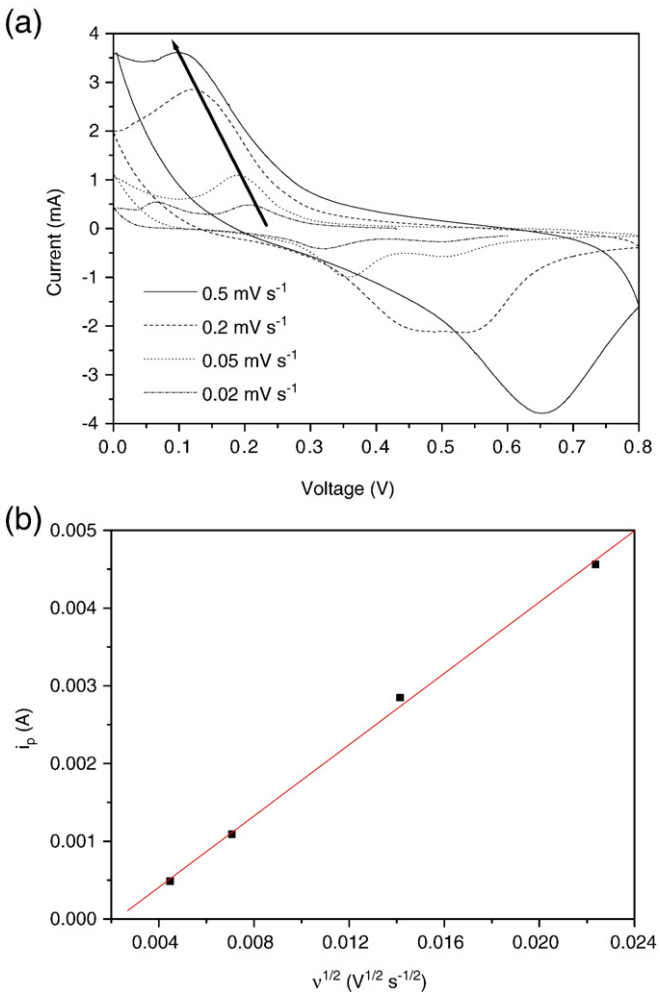

Fig. 3. (a) Cyclic voltammetry curves with different scan rates: 0.02, 0.05, 0.2 and 0.5 mV s^{-1}; (b) The relationship of the peak current (i_p) and the square root of scan rate ($\nu^{1/2}$).

the model proposed by Ho et al. [23], according to the following equation:

$$D_{Li^+} = 1/2[(V_M/SFA)(\delta E/\delta x)]^2 \quad (2)$$

where V_M is the mole volume of silicon, F is the Faraday constant (96,486 C mol^{-1}), A is the plot slope of imaginary resistance ($Z_{im.}$) vs.

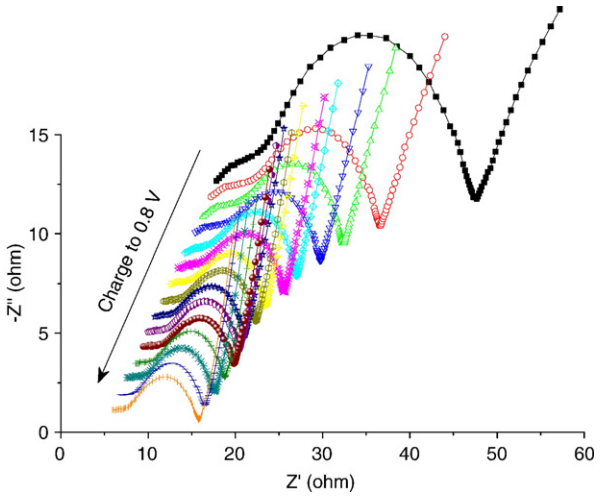

Fig. 4. Nyquist plots of nano-Si at different charge states.

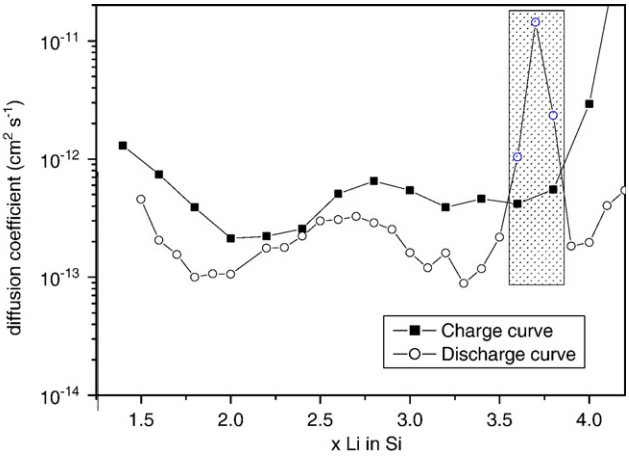

Fig. 5. Diffusion coefficients of lithium ions in nano-Si calculated from EIS.

inverse square root of angular frequency $\left(1/\sqrt{2\pi f}\right)$, which can be obtained from the Warburg impedance, and $\delta E/\delta x$ is the slope of galvanostatic charge–discharge curves.

Fig. 5 shows the diffusion coefficients of lithium ions obtained from Eq. (2). D_{Li^+} is about 10^{-12} cm^2 s^{-1}. This value is quite consistent with the result calculated from CVs. In addition, the variation of D_{Li^+} with x in Li_xSi exhibits a "W" type with two minimum regions at $Li_{2.1\pm0.2}Si$

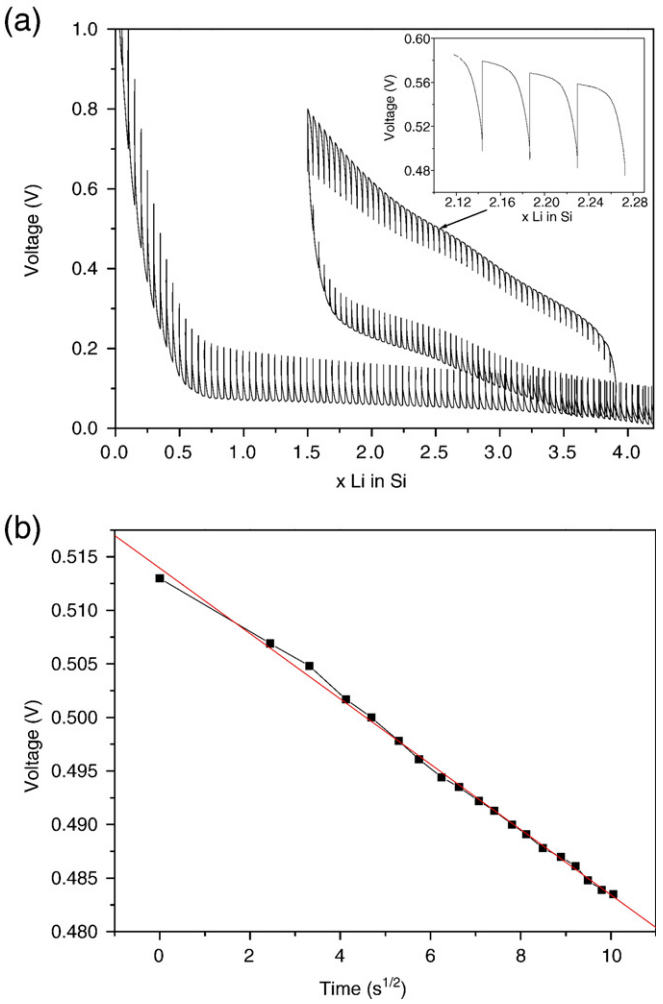

Fig. 6. (a) Galvanostatic intermittent titration curve of nano-Si with a pulse of 50 mA g^{-1}; (b) The relationship of voltage change and the square root of interrupt time.

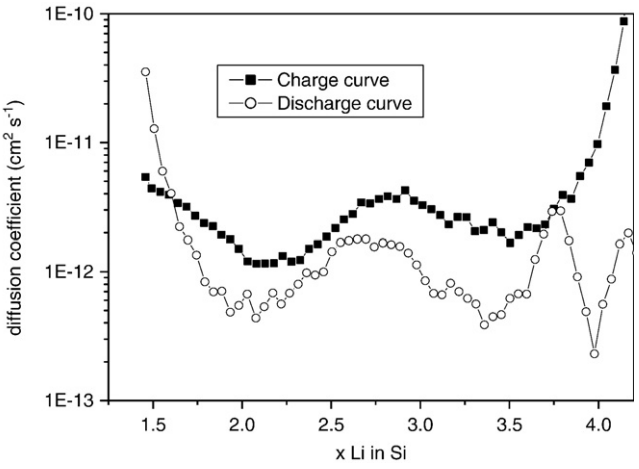

Fig. 7. Diffusion coefficients of lithium ions in nano-Si calculated from GITT.

and $Li_{3.2\pm0.2}Si$, these two minimum regions of D_{Li^+} are related to the strong attractive interactions between lithium and the host matrix [24]. Though both X-ray diffraction (XRD) and high resolution transmission electron microscope (HRTEM) studies have not found any crystalline phases at $x<3.75$ [7], the two minimum regions ($Li_{2.1}Si$ and $Li_{3.3}Si$) seem to coincide with the two crystalline phases (Li_7Si_3 and $Li_{13}Si_4$) formed at 400 °C, hence they are noted here as a-Li_7Si_3 and a-$Li_{13}Si_4$. Recently, Li et al. have announced that there is an amorphous phase ($Li_{2.0}Si$) coexisting with $Li_{15}Si_4$ with x ranging from 2 to 3.75 [11]. In our studies, it is found that besides the amorphous composition of a-$Li_{2.0}Si$, there is another composition of a-$Li_{13}Si_4$. It is also observed that D_{Li^+} varies drastically with x in the range of 3.6–3.8, corresponding to the formation of crystalline $Li_{15}Si_4$. However, the Warburg part of EIS seems to be not distinct enough in this range, which enlarges the calculation errors. More reliable D_{Li^+} is calculated from galvanostatic intermittent titration (GITT).

Assuming that lithium transport in the electrode obeys Fick's second law and according to the equation derived by Weppner and Huggins [25], the diffusion coefficients of lithium ions can also be calculated as the following equation:

$$D_{Li^+} = 4/\pi(V_M/SF)^2 \times \left[I^0(\delta E/\delta x)/\left(\delta E/\delta t^{1/2}\right)\right]^2 \quad (3)$$

In Eq. (3), the Warburg related parameter A is replaced by $\delta E/\delta t^{1/2}$, the slope of voltage change vs. the square root of interruption time, which can be directly obtained from GITT curve. Fig. 6a shows the GITT curve of nano-Si. Fig. 6b displays that the voltage change has a good linearity with the square root of interruption time.

Fig. 7 shows the diffusion coefficients of lithium ions in nano-Si calculated from GITT. D_{Li^+} calculated from GITT is about 5 times higher than that calculated from EIS. The difference is due to the results obtained in different equilibrium conditions. In comparison with the GITT results, the EIS results were obtained under more equilibrium conditions and the electrode has more time for relaxation. Nonetheless, the results calculated from EIS or from GITT show the same variation type with the lithium concentration in silicon. The variation of D_{Li^+} calculated from GITT also exhibits a "W" type with two minimum regions at $Li_{2.1\pm0.2}Si$ and $Li_{3.2\pm0.2}Si$. In the x (Li_xSi) range from 3.5 to 4.0, D_{Li^+} has a large fluctuation. Similar phenomenon that between the two minima D_{Li^+} at $Li_{0.53}CoO_2$ and $Li_{0.48}CoO_2$, is a maximum D_{Li^+} at $Li_{0.5}CoO_2$, has also been observed by Jang et al. in the study of D_{Li^+} in Li_xCoO_2 ($0.45<x<0.7$) [26]. Because the phase transition of $LiCoO_2$ in the whole charging process has been well studied, the region of the minima in D_{Li^+} in Li_xCoO_2 ($0.45<x<0.7$) corresponds to the phase boundaries of the Li vacancy ordered phase [27,28]. Back to the lithium intercalation in silicon, there is a crystalline phase when x in Li_xSi reaches 3.75 ($Li_{15}Si_4$) confirmed by the ex-situ/in-situ X-ray diffraction studies. Therefore this fluctuation is related to the formation of crystalline $Li_{15}Si_4$ [29]. It should be mentioned that the formation of crystalline $Li_{15}Si_4$ can only be observed in the discharge process. The galvanostatic charge curve only exhibits two plateaus, corresponding to a-Li_7Si_3 and a-$Li_{13}Si_4$, respectively. D_{Li^+} values calculated from the charge curve also lose its fluctuation at around $Li_{15}Si_4$. The reason is probably due to the large impedance (as shown in Fig. 4). Though XRD study has shown that the diffraction peaks of crystalline $Li_{15}Si_4$ disappear in the next charge process [11], the cyclability of nano-Si can be significantly enhanced by setting a higher cut-off voltage to avoid the formation of crystalline $Li_{15}Si_4$ [30].

4. Conclusions

The diffusion coefficients of lithium ions in nano-Si at different charge–discharge states are determined by EIS and GITT. D_{Li^+} values calculated from EIS range from 10^{-13} to 10^{-12} cm^2 s^{-1}. The results calculated from GITT are a little higher than that from EIS due to its non-equilibrium states. These results fit the apparent diffusion coefficient of lithium ions (5.1×10^{-12} cm^2 s^{-1}) calculated from CVs very well. D_{Li^+} varies with the lithium concentration in silicon and exhibits a "W" type. Two amorphous composition, a-Li_7Si_3 and a-$Li_{13}Si_4$ are proposed existence during charge and discharge. Besides the two minimum regions, one maximum D_{Li^+} is observed at $Li_{15}Si_4$, corresponding to the formation of crystalline $Li_{15}Si_4$.

Acknowledgements

This research was supported by National Science Foundation of China (grant No. 20471057). N. Ding gratefully thanks the joint doctoral promotion program launched between Chinese Academy of Sciences (CAS) and Max Planck Institute (MPI).

References

[1] U. Kasavajjula, C.S. Wang, A.J. Appleby, J. Power Sources 163 (2007) 1003.
[2] R.A. Huggins, J. Power Sources 81–82 (1999) 13.
[3] T. Kubota, T. Tanaka, Jpn. Kokai Tokkyo Koho, JP 94-55614-940325 (1994).
[4] E. Funatsu, Jpn. Kokai Tokkyo Koho, JP 94-2592-940114 (1994).
[5] B.A. Boukamp, G.C. Lesh, R.A. Huggins, J. Electrochem. Soc. 128 (1981) 725.
[6] W.J. Weydanz, M. Wohlfahrt-Mehrens, R.A. Huggins, J. Power Sources 81–82 (1999) 237.
[7] H. Li, X.J. Huang, L.Q. Chen, G.W. Zhou, Z. Zhang, D.P. Yu, Y.J. Mo, N. Pei, Solid State Ionics 135 (2000) 181.
[8] H.J. Jung, M. Park, Y.G. Yoon, G.B. Kim, S.K. Joo, J. Power Sources 115 (2003) 346.
[9] M. Holzapfel, H. Buqa, L.J. Hardwich, M. Hahn, Electrochim. Acta 52 (2006) 973.
[10] M.N. Obrovac, L.J. Krause, J. Electrochem. Soc. 154 (2007) A103.
[11] J. Li, J.R. Dahn, J. Electrochem. Soc. 154 (2007) A156.
[12] Z.S. Wen, J. Yang, B.F. Wang, K. Wang, Y. Liu, Electrochem. Commun. 5 (2003) 165.
[13] N. Dimov, S. Kugino, M. Yoshio, Electrochim. Acta 48 (2003) 1579.
[14] S. Ohara, J. Suzuki, K. Sekine, T. Takamura, J. Power Sources 119–121 (2003) 591.
[15] Il-Seok Kim, P.N. Kumta, J. Power Sources 136 (2004) 145.
[16] Y. Liu, K. Hanai, J. Yang, N. Imanishi, A. Hirano, Y. Takeda, Solid State Ionics 168 (2004) 61.
[17] S.-H. Ng, J. Wang, D. Wexler, K. Konstantinov, Z.-P. Guo, H.-K. Liu, Angew. Chem., Int. Ed. 45 (2006) 6896.
[18] K. Dokko, M. Mohamedi, Y. Fujita, T. Itoh, M. Nishizawa, M. Umeda, I. Uchida, J. Electrochem. Soc. 148 (2001) A422.
[19] Y.H. Rho, K. Kanamura, J. Electrochem. Soc. 151 (2004) A1406.
[20] P.P. Prosini, M. Lisi, D. Zane, M. Pasquali, Solid State Ionics 148 (2002) 45.
[21] T.L. Kulova, A.M. Skundin, E.A. Nizhnikovskii, A.V. Fesenko, Russ. J. Electrochem. 43 (2006) 300.
[22] E.M. Pell, Phys. Rev. 119 (1960) 1222.
[23] H. Xia, L. Lu, G. Ceder, J. Power Sources 159 (2006) 1422.
[24] C. Ho, I.D. Raistrick, R.A. Huggins, J. Electrochem. Soc. 127 (1980) 343.
[25] W. Weppner, R.A. Huggins, J. Electrochem. Soc. 124 (1977) 1569.
[26] Y-Il Jang, B.J. Neudecker, N.J. Dudney, Electrochem. Solid-State Lett. 4 (2001) A74.
[27] J.N. Reimers, J.R. Dahn, J. Electrochem. Soc. 139 (1992) 2091.
[28] X.Q. Yang, X. Sun, J. McBreen, Electrochem. Commun. 2 (2000) 100.
[29] T.D. Hatchard, J.R. Dahn, J. Electrochem. Soc. 151 (2004) A838.
[30] Y.-M. Kang, S.-M. Lee, S.-J. Kim, G.-J. Jeong, M.-S. Sung, W.-U. Choi, S.-S. Kim, Electrochem. Commun. 9 (2007) 959.